Recent progress in ultrasound-mediated cancer therapeutics with micelles and liposomes: a review

Debasmita Mukhopadhyay,[1] Catherine Sano,[2] Nour AlSawaftah[1], Vinod Paul[1], Rafat El-Awadi[3], Ghaleb A Husseini[1,]*

[1]Chemical Engineering Department, American University of Sharjah, Sharjah, UAE

[2]Chemical Engineering Department, University of Virginia, Charlottesville, VA, USA

[3]College of Pharmacy, University of Sharjah, Sharjah, UAE

Abstract

Nanoparticles have proven promising as cancer theranostic tools. Nanoparticles are selective in nature, have reduced toxicity, and controllable drug release patterns making them ideal carriers for anticancer drugs. Numerous nanocarriers have been designed to combat malignancies, including liposomes, micelles, dendrimers, and, more recently, metal organic frameworks. The temporal and spatial release of therapeutic agents from these nanostructures can be controlled using internal and external triggers, including pH, enzymes, redox, temperature, magnetic and electromagnetic waves, and ultrasound. Ultrasound is an attractive modality because it is non-invasive, can be focused on the diseased site, and has a synergistic effect with anticancer drugs. This review will focus on the use of ultrasound-mediated liposomes and polymeric micelles in cancer therapy.

Keywords: Nanomedicine, liposomes, polymeric micelles, drug delivery, ultrasound, cancer therapy.

1. Introduction

Cancer, one of the leading causes of mortality globally, is characterized by an abnormal and uncontrollable growth of cells, forming tumors (*1*, *2*). Treatment options depend on the stage of cancer development. In its early stages, surgery and radiation are often used to eradicate local tumors (*3*). However, these methods are ineffective for late-stage cancers, especially when metastasis has occurred. In advanced cancers, chemotherapy is the primary choice of treatment (*4–9*). Chemotherapy uses powerful chemicals to kill fast-growing cells. It is given to patients with a curative intent or to prolong life and/or reduce symptoms(*10*, *11*).

* Corresponding author: ghusseini@aus.edu

"The published manuscript is available at EurekaSelect via http://www.eurekaselect.com/ [https://doi.org/10.2174/1574892816666210706155110].

The main limitation of chemotherapy is its lack of selectivity, as it affects healthy and malignant cells indiscriminately. As a result, chemotherapy has many undesirable and often severe side effects such as fatigue, hair loss, anemia, nausea, fertility problems, and other side effects that significantly reduce the quality of life of cancer patients (*12–15*). Nanoscale (10-200 nm) smart drug delivery systems can be utilized to minimize the chemotherapeutic side effects while enhancing the efficacy of the treatment (*16–21*). Nanocarriers include liposomes, micelles, shelled vesicles, solid lipid particles, quantum dots (QDs), carbon nanotubes (CNTs), metal organic frameworks (MOFs), etc. Loading anticancer drugs into nanocarriers can reduce their toxicity and associated side effects, increase their stability, extend their blood circulation time, and allow for controlled drug release. Moreover, their nanoscale size allows them to accumulate at the tumor site due to the irregular nature of tumor endothelia, a phenomenon known as the enhanced permeability and retention (EPR) effect (*22–25*).

In this article, we will review key advances in liposomes and polymeric micelles, and their role in ultrasound-mediated drug delivery to cancerous tissues.

1.1. Ultrasound mediated drug delivery

Ultrasound (US) waves are mechanical waves with frequencies higher than the audible range (>20 kHz). Due to its nonionizing and non-invasive nature, US found numerous applications in the medical field, e.g., imaging, lithotripsy, focused US surgery, and tumor ablation. US has also shown great promise in the field of targeted drug delivery, particularly cancer (*26*, *27*). US is advantageous in drug delivery because it (*28*, *29*):

1. Amplifies the release of the drug: US or acoustically-activated drug delivery utilizes the thermal (hyperthermia) and mechanical properties of US (cavitation and micro-streaming) to amplify/enhance/trigger drug release (*30*) (*31*). One of chemotherapy's primary limitations is its nonspecific therapeutic effect resulting in damage to healthy and cancerous cells. To overcome this shortcoming, US-mediated drug delivery

specifically focuses acoustic power on the targeted diseased area, thus enhancing drug release and specificity (*32*).

2. Facilitates specific drug accumulation at the targeted site: Multidrug resistance (MDR) is a major challenge in cancer treatment, which can limit the effectiveness of chemotherapy and is responsible for the overall low efficacy of drug therapies. Several mechanisms contribute to MDR including, membrane efflux pumps (namely ATP-binding cassette (ABC) transporter proteins), mutations of oncogenes rendering them resistant to chemotherapeutic treatments, the ability of cancer cells to adapt and manipulate their microenvironment such that it supports their growth, survived cancer stem cells (CSCs) that resist conventional therapies, and activated cell growth factors (*33*, *34*). Recently, the use of nanoparticles (NPs) as drug delivery systems has been investigated to overcome the MDR phenomenon in solid tumors. Studies have shown that the US enhances the permeability of tumor tissues and mediates the disruption of NPs, hence releasing the drug and exposing cancer cells to these anti-neoplastic agents (*35*) (*31*).
3. Enhances the permeability of NPs, hence aiding in the release of their therapeutic contents: The most significant limitation in nanoparticle-mediated chemotherapy is insufficient and uneven uptake of nanocarriers into tumor tissues (*36*). US-induced hyperthermia can help increase the uptake of nanocarriers by increasing the permeability of tissues and vessels in the tumor. In addition, shock waves and micro-jets caused by the collapse of cavitation bubbles, i.e., sonoporation, can generate pores in the tumor vasculature, which enhance the extravasation of nanocarriers and subsequent delivery of therapeutics to the tumor site (*27*, *34*).

1.2. Ultrasound-sensitive nanoparticles

The use of US as a triggering mechanism for NPs shows promise in cancer treatment applications because it is non-invasive, and facilitates the specific delivery of

chemotherapeutics to tumor sites thus minimizing the adverse systemic side effects on healthy tissues, refer to Figure 1. Release from US-responsive nanocarriers can be due to the thermal effects of US, mechanical effects of US, or a combination of both (*26*). Several studies have reported how US and NP interactions can trigger various cellular pathways, which can be therapeutically exploited. The following discussion presents examples of the research work focused on US-responsive nanocarriers in cancer therapy, with a special focus on US-triggered micelles and liposomes (*19*, *21*, *37–41*).

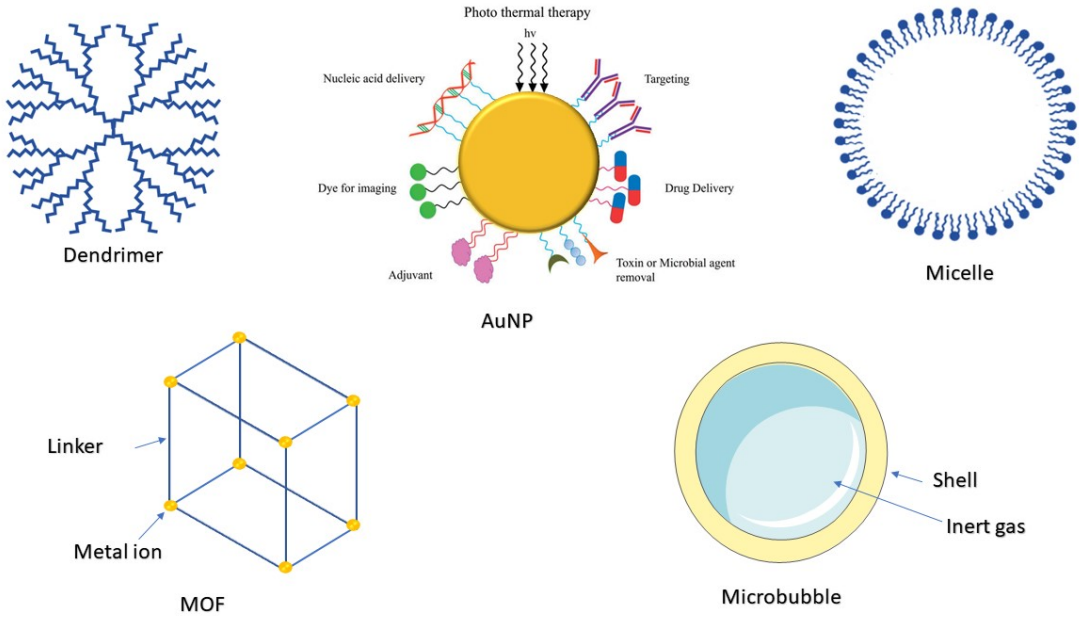

Figure 1. Types of nanocarriers

1.2.1. Ultrasound-responsive dendrimers

Dendrimers are hyperbranched, nanosized molecules consisting of a core from which dendrons (branches of other atoms) are projected through various chemical reactions (*42*). Drugs, and other materials can be incorporated into dendrimers through several methods such as encapsulation, conjugation, or complexation. Drug-dendrimer complexes have shown drug delivery capabilities because of their high solubility, reduced systemic toxicity, and selective accumulation in solid tumors [18]. In a study by Huang et al. (*43*), a polyamidoamine

dendrimer coupled with sonophoresis was used to improve the transdermal absorption of diclofenac (DF). The DF permeation study results showed that the developed system has the potential to enhance the permeation of DF through the skin. The cumulative drug permeated through the skin was 56.69 μg/cm^2 for the DF gel alone, 257.3 μg/cm^2 for the DF-dendrimer complex without sonophoresis, and 935.21 μg/cm^2 for the DF-dendrimer system with sonophoresis after 24 hours. Manikkath et al. (*44*) demonstrated enhanced transdermal permeation of PAMAM dendrimers delivering ketoprofen with low-frequency ultrasound (LFUS).

1.2.2. Ultrasound-responsive gold nanoparticles

Gold nanoparticles (Au NPs) are nanosized gold particles that have been widely employed in bio-nanotechnology applications. Due to their biocompatibility, ability to permeate through skin, and capacity to generate heat with laser excitation, Au NPs have shown great promise as drug delivery vehicles (*45*). A study by Kang et al. (*46*) utilized Au NPs coupled with DNA, aptamers, and doxorubicin (DOX) for US-mediated targeted drug delivery. Enhanced cellular uptake of DOX was observed with the treatment of high-intensity focused ultrasound (HIFU). Another study by Brazzale et al. (*47*) investigated the use of Au NPs coated with PEG and folic acid (FA-PEG-GNP) to target two cancer cell lines (KB and HCT-116), followed by exposure to US at 1.866 MHz for 5 min. The *in vitro* studies showed significantly reduced cell growth and proliferation together with the significant generation of reactive oxygen species (ROS).

1.2.3. Ultrasound-responsive metal organic frameworks

Metal organic frameworks (MOFs) are self-assembling metal ions surrounded by organic ‘linker’ molecules. MOFs have high loading capacities and are biocompatible and hence are candidates for drug delivery applications. Ibrahim et al. (*48*) synthesized a new MOF using iron nitrate and 2,6-naphthalenedicarboxylic acid using two methods, microwave irradiation (Fe-NDC-M) and solvothermally using a conventional electric oven (Fe-NDC-O). The results of the characterization tests indicated that the synthesized Fe-NDC-MOFs are within the size

range to take advantage of the EPR effect, and hence could be useful as a drug carrier system. A study by Pan et al. (*49*) utilized porphyrin-like metal centers (PMCS) to increase the sonosensitivity of a MOF-derived carbon nanostructure. The occurrence of acoustic cavitation was caught by high-speed camera and was attributed to cavitation bubbles and microjets. The MOF and US treatment resulted in an 85% tumor inhibition efficiency, creating a promising mode of cancer therapy.

1.2.4. Ultrasound-responsive microbubbles

US and gas-encapsulated microbubbles can be utilized to temporarily form pores and enhance the permeability across biological barriers such as vessel walls, cell membranes, and the blood brain barrier (BBB), in a process known as sonoporation (*50*). Treat et al. (*51*) exhibited reduced tumor growth and prolonged survival times in US-mediated microbubble treatment with DOX in a mouse brain tumor model. Ting et al. (*52*) validated the results of Treat et al. (*51*); his study reported minimized systemic drug toxicity. Despite promising *in vivo* results, the specific mechanism of sonication and microbubble drug delivery have yet to be applied clinically.

1.2.5. Ultrasound-responsive micelles

Micelles are unilamellar vesicles made of amphiphilic polymeric molecules with a hydrophobic core hidden inside the structure and a hydrophilic shell directed outwards with a size range of 10-100 nm (*53*, *54*). Drugs can be loaded into micelles either through chemical covalent bonding or through physical encapsulation. (*55–57*). Micelles have many advantages as drug delivery carriers, including ease of preparation, stability under physiological conditions, prolonged shelf-life, extended circulation time in blood and biological fluids, increased bioavailability, and enhanced pharmacokinetics and biodistribution properties. Polymeric micelles (PMs) spontaneously form from amphiphilic copolymers when dispersed in aqueous media and have been extensively researched for the delivery of hydrophobic drugs (*58–62*). PMs have several advantages over surfactant micelles, such as enhanced stability,

longer retention times, and controlled drug release. Block copolymer micelles are a promising class of MPs formed by conjugating a homopolymer to one or more homopolymers. In addition, PMs composed of Pluronic® block copolymers have gained special attention in cancer drug delivery because they can inhibit P-glycoprotein (Pgp)-mediated efflux, a process associated with MDR. Examples of PMs formed using Pluronic® block copolymers include triblock copolymers of poly (ethylene oxide) (PEO) and poly (propylene oxide) (PPO), often denoted by PEO-PPO-PEO (*63*).

To enhance the interactions between PMs and tumor cells, a wide variety of targeting molecules can be used to functionalize their surfaces. Targeting molecules include proteins (e.g., transferrin, albumin, and affibodies), peptides (e.g., F3 peptide, RGD, sKLWVLPK, and aptides), antibodies and antibody fragments (F(ab)/2, F(ab/), and scFv), small molecules (e.g., folic acid), and nucleic acid-based ligands such as the A10 and A9 CGA aptamers (*55*).

1.2.6. Ultrasound-responsive exosomes

Exosomes are small (with a size range of 40–160 nm) extracellular vesicles involved in various biological processes (*64*). Exosomes are composed of different lipids and proteins derived from the parent cells. Moreover, the composition of exosomes and their cargo determine their biological function, the elimination of unnecessary proteins and RNAs, coagulation, inflammation, transfer of horizontal miRNAs and angiogenesis (*64*, *65*). In addition to these biological functions, exosomes are associated with several diseases, including Parkinson's disease, Huntington disease, myocardial infarction, human immunodeficiency virus (HIV), and cancer. Currently, extensive research has been dedicated to utilizing exosomes as drug delivery vehicles. Exosomes are appealing as nano-vehicles because they intrinsically possess the desirable features of an ideal drug delivery system, such as a long-circulating half-life, specificity, biocompatibility, stability in blood and serum, ability to deliver their cargo to specific targets over a long distance, reduced clearance rate, facilitated cellular uptake and minimal or no inherent toxicity issue (*65*, *66*).

Several studies have explored the use of exosomes as drug delivery systems; for instance, Sun et al. (*67*) investigated UTMD assisted exosome delivery to the heart, adipose tissue, and skeletal muscles. DiR-labeled exosomes with/without UTMD of SonoVue^{TM} microbubbles were injected into the tail vein of mice and followed by *in vivo* and *ex vivo* tracking of these nanocarriers. Fluorescence imaging and confocal laser scanning microscopy showed that the targeted destruction of SonoVue^{TM} microbubbles using US significantly increased exosome endocytosis in the heart and adipose tissue region. Liu et al. (*68*) studied the use of sonodynamic therapy to guide the delivery of homotypic tumor cell-derived exosomes loaded with sinoporphyrin sodium (EXO-DVDMS). Results showed that EXO-DVDMSs enabled the simultaneous imaging and tumor metastasis inhibition, which were found to be 3-fold and 10-fold higher than that of free DVDMS, respectively.

1.3. Ultrasound-responsive micelles in cancer therapy

US is a powerful modality for spatial and temporal control of drug delivery. As mentioned earlier, US-mediated release from nanocarriers occurs as a response to either the thermal or cavitational effects of US. Hydrophobic drugs are encapsulated in the micellar core which is held together by hydrophobic interactions; therefore, an increase in temperature would strengthen these bonds; therefore, a different approach is needed to imbue micelles with temperature responsiveness. One way to address this issue involves incorporating thermo-responsive blocks, such as poly(N-alkylacrylamide) compounds into the micellar structure. Another approach consists of polymerizing temperature-responsive lower critical solution temperature (LCST) hydrogels inside micellar cores (*26*, *69*).

With respect to release induced by the cavitational effects of US, Pitt, Rapoport, Husseini et al. (*70*) pioneered the work in the field of US-mediated micellar drug delivery (*28*, *29*),(*71–74*). Rapoport and Pitt (*75*) studied US-triggered drug delivery from Pluronic P105 PMs. The results showed that US triggering of micelles could help reduce the adverse side effects associated with the high doses of the chemotherapeutics usually administered to cancer

patients. In another study, Pitt, Husseini, and Kherbeck (*76*) investigated LFUS-induced DOX release from folate-conjugated Pluronic P105 micelles. The results showed that the percent drug release increases with increasing US power intensity. The studies above have reported on the 'physical' release mechanism of micelles triggered by acoustic cavitation. They observed that in the absence of US, micelles reassemble, re-encapsulating their payload in the process (*77*). Pitt, Rapoport, Husseini et al. (*78*) also studied the administration of different stabilized and non-stabilized micelles on several cancer cell lines. Furthermore, Husseini et al. (*73*) used real-time fluorescence detection to monitor the acoustically prompted release of drugs from PMs under continuous and pulsed US in a frequency range of 20–90 kHz. Marin et al. (*79*, *80*) also studied the effect of continuous-wave and pulsed US on DOX uptake by HL-60 cells from PM solutions. When sonicated, micelles released their contents due to the presence of collapsing bubbles; the drugs were later re-encapsulated when the US was turned off. In another study by Marin et al. (*81*), a significant amount of release was observed when high-intensity focused ultrasound (HIFU) was applied to DOX-loaded micelles. Additionally, Husseini et al. (*72*, *81*, *82*) investigated the role of cavitation in US-triggered drug delivery, and their findings confirmed that cavitation was behind the release phenomenon (*72*). Contrastingly, Diaz de la Rosa et al. (*83*) observed no DOX release from non-stabilized micelles at 500 kHz. Another research group (*84*) found that LFUS was capable of releasing hydrophobic markers from PMs in a better fashion than that induced by the thermal effect.

Stevenson-Abouelnasr et al. (*85*, *86*) conducted studies to determine the mechanism and kinetics of DOX release from Pluronic P105 micelles in the presence of US; and proposed the following mechanism: micelle destruction, destruction of cavitating nuclei, reassembly of micelles, followed by the re-encapsulation of DOX. Staples et al. (*87*) investigated DOX release from Pluronic P105 micelle using two different US frequencies (namely, 20 kHz and 476 kHz) in colorectal epithelial cell line as well as in a xenograft rat model. Combining US

application with micelles was effective in reducing the tumor growth rate, at both tested frequencies.

Regarding carrier design, a major drawback for P105 micelles is their instability upon dilution. To overcome this issue, Rapoport et al. (*88*) proposed three solutions: (1) the radical crosslinking of micelle interiors; (2) introducing vegetable oil into the Pluronic solutions, and (3) the polymerization of temperature receptive LCST hydrogel in the core of PMs, termed NanoDeliv™. Out of these three solutions, dense Plurogel micelles showed the most significant increase in uptake of drugs in the presence of US waves. Husseini et al. (*81*, *82*, *89*) prepared P105 micelles with N,N-diehtylacrylamide, NanoDeliv™ . The results revealed that stabilized micelles released almost 2% DOX within two seconds of exposure to 70 kHz US (*90*). Zeng and Pitt (*91*) prepared PMs made up of an amphiphilic copolymer, poly(ethyleneoxide)-b-poly(N-isopropylacrylamide-co-2-hydroxyethyl methacrylate-lactate$_{n)}$. The synthesized micelles had a half-life of about 48 hours at 40 °C and were able to release around 4 % of their DOX content at body temperature upon exposure to US. Another study from Husseini et al. (*92*) established that US with frequencies between 70 and 476 kHz can disrupt the covalent networks of stabilized NanoDeliv^{TM} micelles. However, there was no statistically significant difference in release after US exposure at both frequencies. In 2013, Husseini et al. (*93*) determined that folate-targeted Pluronic P105 micelles encapsulating DOX could acoustically release almost 14 % of the drug when insonated. Chen et al. (*94*) reported that Pluronic mixed micelles consisting of Pluronic P105 and F127 enhanced the antitumor activity of methotrexate (MTX) and are promising drug delivery platforms for MDR modulation in the MDR tumor cells A-549 and KB cells and the sensitive tumor cells H-460. Another study reported that encapsulated curcumin was released from Pluronic P123/F127 micelles by focused ultrasound, resulting in US-triggered drug release with a longer circulation time and increased cellular uptake, which translated to more than a six-fold tumor regression in the *in vivo* model (*95*).

Sonodynamic therapy (SDT) is a treatment against solid tumors combining a sonosensitive drug and HIFU to generate cytotoxic ROSs in and around cancer cells. In 2017, Maeda et al. (*96*) developed anticancer micelles, NC-6300, loaded with Epirubicin (EPI) through an acid-labile hydrazone bond. The developed system exhibited antitumor effects upon triggering with low energy HIFU in mouse models. Horise et al. (*97*) studied the efficiency of NC-6300 micelles and high-frequency ultrasound (HFUS) in treating spontaneous tumors in pet dogs. The US parameters used were 1-MHz frequency with a focal length of 120 mm, an outer diameter of 120 mm, and an inner diameter of 40 mm. The results showed that anticancer micelles, NC-6300, encapsulating EPI accumulated in tumor cells via ROS generation and the enhanced permeability and retention (EPR) effect. Another study detailed combing NC-6300 and HIFU as a useful approach for the production of hydroxyl radicals was enhanced with TP-HIFU (at a frequency of 1.09 MHz) (*98*). The infrared spectroscopic investigation of US-mediated disruption of micelles composed of a diblock copolymer demonstrated the occurrence of carboxylic acid dimers and hydroxyl groups, which involved the cleavage of THP groups by HIFU triggered hydrolysis. The interruption of PEO-b-PTHPMA micelles by US further showed the potency of HFUS at penetrating block copolymer micelles with labile chemical bonds (*37*).

In 2009, a new concept was developed for drug release using US; this concept involved the irreversible release of the micellar payload through US-mediated chemical disruption of micelles (*99*). In this method, micelles comprised of amphipathic block copolymers are degraded by US exposure because the latter creates an imbalance between the hydrophobic and hydrophilic structure of micelles, hence releasing the internalized payload. Zhang et al. (*99*) synthesized micelles composed of the amphiphilic block copolymer PLA-b-PEG encapsulating the model drug Nile Red. HIFU was used as a contactless and remote-controlled method to triggering the release of the entrapped Nile Red from micelles. The irreversible release of Nile

Red from the developed micellar system was attributed to the degradation of the PLA-b-PEG chain due to transient cavitation events at the HIFU focal spot. Li et al. (*100*) used HIFU to release pyrene from redox-responsive PEG S-S-PLA micelles. When exposed to HIFU, pyrene release reached around 90% in 10 minutes at a power of 80 W, whereas the release was significantly slower when the micelles were exposed to a GSH reducing agent only.

Table I below presents a summary of some studies focused on US-induced drug release from PMs. Non-Pluronic micelles have also been investigated for US-triggered release. Table II presents several relevant studies, while Table III presents micellar anticancer treatments currently undergoing preclinical and clinical trials.

1.4. US-responsive liposomes in cancer therapy

Liposomes are artificial phospholipid vesicles with an aqueous core compartment enclosed by a lipid bilayer membrane. The phospholipids of the bilayer are arranged such that their hydrophobic tails are facing each other while their hydrophilic heads face the aqueous core (*101–103*). The phospholipids making up liposomes can be commonly found in nature, such as in soybean and egg yolks; however, these are difficult to use in clinical settings due to their instability and contamination risks (*104*). Therefore, synthetic phospholipid derivatives such as 1,2 dipalmitoyl-sn-glycerol-3-phosphoglycerol (DPPG), di-palmitoylphosphatidylcholine (DPPC), and hydrogenated soy phosphatidylcholine (HSPC), are favorable to synthesize liposomes (*104*).

Liposomes are biologically inert and biocompatible, rarely produce toxic or antigenic reactions, protect the drugs enclosed within their structure from external factors, and can deliver their contents inside cells and even inside different cell compartments, refer to Figure 4 (*105*, *106*). The three main classifications of liposomes are unilamellar vesicles (ULVs, 25 nm - 1 μm) (*107–109*), multi-lamellar vesicles (MLVs, 0.1-15 μm) (*110*, *111*), and multi-vesicular vesicles (MVVs, 1.6-10.5 μm) (*112–114*). ULV liposomes are further classified into two subcategories,

which are large unilamellar vesicles (LUVs, 100 nm – 1 μm) and small unilamellar vesicles (SUVs, 25-50 nm), refer to Figure 2. The size and lamellarity affect the amount of drug encapsulation in liposomes and the circulation half-life in the body (*115*).

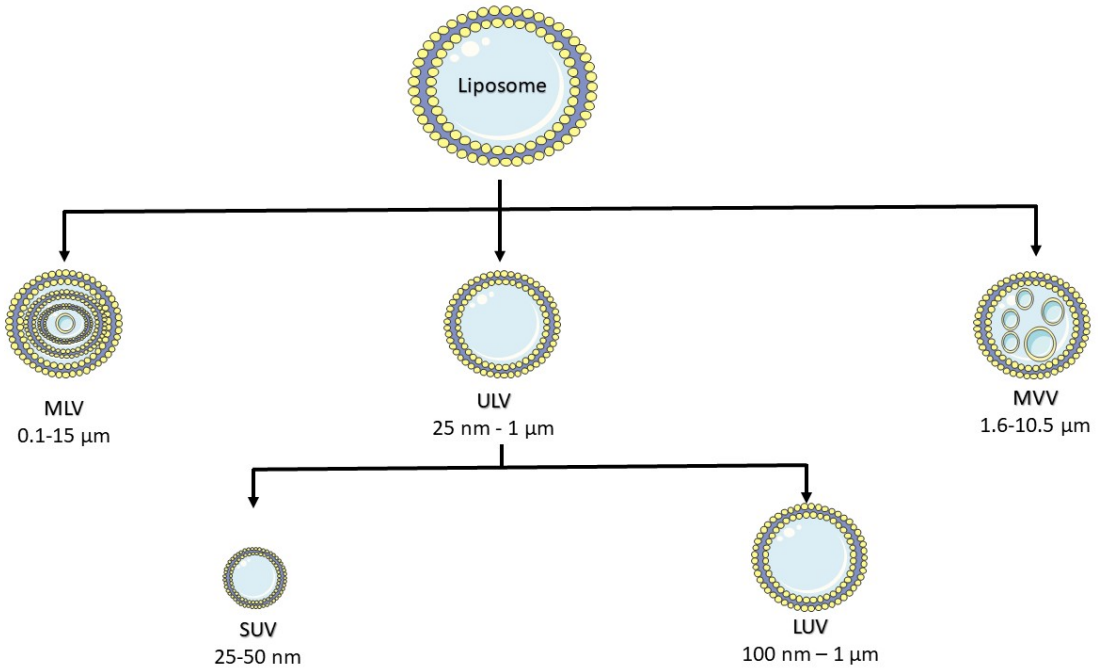

Figure 2. Classification of liposomes based on size and lamellarity.

Although liposomes are considered superior to other drug delivery systems in many ways, they suffer from short circulation times and low biodistribution (*116*) (*117*). The short circulation time of these nanocarriers can be attributed to several factors, including the size and recognition by the immune system. Small liposomes of 5 nm or less can efficiently extravasate into tumor tissue, but are rapidly filtered by the kidneys, drastically decreasing their circulation time (*24*, *118*). Increasing the size of the liposomes enhances their circulation time by slowing down kidney filtration, while still allowing for diffusion into tumor sites via pores and defects in angiogenic vessels (*116*). With regard to recognition by the immune system, since liposomes are foreign bodies, they are susceptible to recognition and tagging by opsonins, which accelerate phagocytosis (*24*). A solution for this problem is coating the surface of the liposome with inert, biocompatible polymers, such as polyethylene glycol (PEG) (*119*).

The bio-distribution of liposomes can be improved by active targeting (conjugating a moiety to the surface of the nanocarriers), which exhibits a specific affinity towards receptors overexpressed on cancer cells, refer to Figure 3 (*120*). Furthermore, the release of liposomal contents can be controlled and enhanced using external stimuli, as the liposomes would circulate throughout the body, but destabilize and release its contents once exposed to a stimulus (*121*). This stimulus could be internal such as pH, temperature, redox agents or the expression of certain enzymes, or external such as temperature, US, light, magnetic and electric field.

Table I. Studies investigating the acoustically triggered drug release from polymeric micelles

Micelle Type	Payload	US parameters	In vitro study	In vivo study	Overview	Ref.
Pluronic copolymer P105	DOX	80 kHz	Human leukemia HL-60	-	• DOX exhibited IC_{50} concentrations of 2.35, 0.9, 1.25, 0.19 μg/ml with DOX, DOX/US, micellar DOX, and micellar DOX/US, respectively.	[122]
Pluronic P105 micelle	DOX and Ruboxyl	70 kHz	Human leukemia HL-60	-	• US enhanced the intracellular uptake of drugs encapsulated in dense PMs in HL60 cells.	[78]
Pluronic P105 micelle	DOX and Ruboxyl	70 kHz	Human leukemia HL-60	-	• Micelles exhibited improved release of drugs upon exposure to US. • Drug re-encapsulation upon cessation of insonation.	[82], [123]
Pluronic micellar solutions	DOX and Ruboxyl	20 kHz	Human leukemia HL-60	-	• The effect of continuous wave and pulsed 20-kHz ultrasound on the DOX uptake by HL-60 cells from PBS and PM solutions was studied.	[79]
Synthesized polymer-cisplatin	Cisplatin prodrug conjugate, Bi (PEG-PLA)-Pt(IV)	-	A2780 human ovarian cancer cells	-	• pH-responsive NPs showed an extremely differential drug release profile at different environmental acidity.	[124]
NC-6300	Epirubicin	1.09 MHz	Human pancreatic cancer cell MIA PaCa-2; & Mouse colon cancer cell (Colon26)	Xenograft mice: CD2 F1/Crlj, 5-wk-old male,	• HIFU triggered micelles increased EPI anticancer effects in mouse models of colon and pancreatic cancer.	[96]
NC-6300	Epirubicin	1 MHz	-	4 different breeds of canines	• NC-6300 micelles incorporating EPI were released by HIFU and accumulated in tumor cells eliciting efficient ROS generation and increased the effectiveness of the SDT treatment.	[97]
NC-6300	Epirubicin	1.09 MHz	Human pancreas adenocarcinoma (BxPC-3) cells; human peripheral promyeloblast (HL-60) cells	-	• Combinatorial treatment with NC-6300 and TP-HIFU increased ROS generation, causing damage to cancer cells.	[98]
Block copolymer PLA-b-PEG.	Nile Red	1.1 MHz	-	-	• HIFU triggered irreversible release of the Nile Red marker from amphiphilic- block copolymer PLA-b-PEG micelles.	[99]

Micelle Type	Payload	US parameters	In vitro study	In vivo study	Overview	Ref.
Pluronic Micelles	DOX	1 MHz	Human leukemia HL-60, ovarian carcinoma drug-sensitive and MDR cells (A2780 and A2780/ADR, respectively), and breast cancer MCF-7 cells.	-	• Enhancement of DOX release of ~8.5 % under HFUS in multiple cancer cells.	[81]
Pluronic micelles	hydrophobic dye NKX-1595	22.8-490 kHz	-	-	• The comparison of US stimulation and thermal stimulation showed higher release from micelles using US.	[84]
Pluronic P105 micelle	DOX	20 kHz, 476 kHz	DHD/K12/TRb colorectal epithelial cell line	Rat model xenograft using colorectal epithelial cell line	• Ultrasound in combination with drug therapy was effective in reducing tumor growth rate, irrespective of which frequency was employed.	[87]
Pluronic P105 micelle	DOX	70 kHz	Human leukemia HL-60	-	• Release of DOX from non-stabilized Pluronic P105 micelles at 37 °C was around 3-times higher than stabilized micelles (10% and 3%, respectively), and they were more susceptible to the shearing forces associated with cavitation.	[90]
Pluronic P105 micelle	DOX	3 MHz, 28 kHz	Breast adenocarcinoma cell line	Female Balb/C mice	• Local sonication with a dual-frequency system caused the drug to release from the micellar carriers and increased drug uptake ability.	[125]
Pluronic P105	DOX	70 kHz, 500 kHz	Human leukemia (HL-60)	-	• A threshold for release between MI =0.35 and 0.40 in was found at 70 kHz and shown to correspond with the appearance of the subharmonic signal in the acoustic spectrum. • Drug release was found to correlate with the increase in subharmonic emission. • No evidence of drug release or a subharmonic signal was detected at 500 kHz.	[83]
Pluronic P105 (Triblock copolymer of PEO_{37}/ PPO_{56}–PEO_{37})	DOX	70-kHz	-	-	• US-triggered P105 micelles which showed a strong correlation between percent drug release and subharmonic acoustic emissions.	[72]
Pluronic P123/F127	Curcumin	1 MHz (*in vitro*), 1.9 MHz (*in vivo*)	Breast cancer cell MDA-MB-231	Female BALB/c mice inoculated with 4T1 cells	• Increased cellular uptake of curcumin corresponding to more than 6-fold tumor regression in an *in vivo* model.	[95]

Micelle Type	Encapsulated substance	US parameters	In vitro study	In vivo study	Overview	Ref.
Stabilized Pluronic P105 micelles	DOX	70 kHz, 476 kHz	Human leukemia (HL-60) cells	-	• US at frequencies 70 and 476 kHz, can disrupt stabilized micellar covalent networks (NanoDeliv ™) • After exposure to 70 kHz and 476 kHz US for 1 h, no significant difference between the network degradation was observed at both frequencies.	[92]
Pluronic-polymeric mixed micelle consisting of Pluronic P105 and F127 block copolymers	Methotrexate	Probe-type ultrasonic treatment (400 W, 10 cycles with 2 second active-3 second duration)	Multidrug resistance tumor cells A-549 and KBv cells & sensitive tumor cells H-460 and KB cells	-	• US Enhanced the antitumor activity of MTX and a promising drug delivery platform for MDR modulation is envisioned.	[94]
Plurogel	DOX & fluorouracil	-	Human colon cancer cell line WiDr	Balb/c nude mice	• US treatment increased the effects of cytostatic drugs on tumor growth. • Synergetic effects were larger for low drug concentrations.	[126]
Plurogel	DOX	20 kHz, 70 kHz	DHD/K12/TRb tumor cell line	BDIX rat model	• Encapsulation of DOX using stabilized PMs and localized release using LFUS showed promise in offering controlled drug delivery in the treatment of tumors in a rat model.	[127]
Fluorescently labelled Pluronic micelles	DOX	1MHz, 3MHz	Ovarian carcinoma A2780 and MDR cells	Male nu/nu mice	• US applied locally to the tumor significantly enhanced the accumulation of PMs in the tumor cells, for unstabilized and stabilized micelles.	[128]
Fluorescently labeled pure and mixed Pluronic P105, PEG2000-diacylphospholipid, and poly(ethylene glycol)-co-poly(h-benzyl-l-aspartate)	DOX	1MHz, 3MHz	Ovarian carcinoma A2780 and MDR cells	Four-week old nu/nu male and female mice	• Local US irradiation of the tumor resulted in substantially increased drug accumulation in tumor cells. • The effect of US was dependent on the time between US application and drug injection. • Due to the US-enhanced drug intracellular uptake and cell killing, the yield of intraperitoneal ovarian carcinoma tumors decreased from 70% for positive control to 36% for DOX encapsulated in PMs combined with a 30-s sonication.	[129]

Micelle Type	Encapsulated substance	US parameters	In vitro study	In vivo study	Overview	Ref.
Fluorescently labelled Pluronic P105	-	1 MHz	Ovarian carcinoma A2780 cells	Immuno-compromised athymic male nu/nu mice	• US interactions with viable cells in the absence and presence of drug carriers and anticancer drugs.	[130]
Amphiphilic poly(ethylene glycol)-block-poly(propylene glycol) copolymer	1, 2, 3-triazole moiety	-	-	-	• PEG-click-PPG micelles triggered the release of the payload following sonication using HIFU involving site-specific ester bond degradation.	[131]
Amphiphilic copolymer, poly(ethylene oxide)-bpoly(N-isopropylacrylamide-co-2-hydroxyethyl methacrylate-lactate n)	DOX	70 kHz	-	-	• DOX release was ~ 4 % at body temperature under US, and the drug was returned to polymeric micelles when insonation ceased.	[91]
PEGylated micelles	Cy5	1.1 MHz	-	-	• HIFU triggered drug release from pH-responsive PEGylated micelles and improved drug uptake *in vitro*.	[132]
Metal supramolecular diblock copolymer (PPG-[Cu]-PEG)	Pyrene, Nile red	1.1MHz	-	-	• The weak Cu (II)−terpyridine dynamic bond in the copolymer chain can be cleaved using US, leading to the disruption of the copolymer micelle and the release of loaded cargo.	[133]
Pluronic P105 micelles with a folate-targeting moiety	DOX	70 kHz	Human cervical cancer cells (KB cells) & W1-38 fibroblasts	-	• The maximum amount of release reached ~ 14 % at an US power density of 5.4 W/cm^2.	[93]
Diblock copolymer (PEO-b-PTHPMA)	-	1.1 MHz	-	-	• The infrared spectroscopic analysis of US-triggered micelles detected the presence of carboxylic acid dimers and hydroxyl groups, suggesting that HIFU could induce the hydrolysis reaction at room temperature resulting in the cleavage of THP groups.	[37]
Block copolymer (PEG-S-S-PLA	Marker	-	-	-	• Fine-tuning of the release kinetics of the encapsulated cargo from the micelles was achieved using HIFU and a redox agent.	[100]
Pluronic copolymer micelle type (PEG-COO-SS-PPG)	Pyrene	HIFU treatment at 70 W	-	-	• Mechanophore sensitivity to US is dependent upon the environmental media. • Under HIFU treatment, up to ~80 % pyrene was released in 10 min, much faster than under DTT treatment.	[134]

Table II. Overview of Non-Pluronic Ultrasound-Responsive Micelles

Micelle Name	Encapsulated substance	Study type/ Effect	Ref.
PEG-co-PLAtocopherol	DOX	Improved drug uptake after 30 s of US application (1 MHz) in mice and the regression of drug-resistant breast cancer (MCF7/ADM) tumors	[135]
PEG-b-PBLA	DOX	8-fold increase of intracellular DOX uptake after 30 s ultrasound application (1 MHz) SK-OV-3 cells	[136]
PEO-b-PTHPMA	-	The application of 1-MHz ultrasound resulted in the hydrolysis of acetal bonds and the cleavage of THP groups	[37]
PEG-b-PLLA	-	The irreversible break of the PEG and PLA linkage after ultrasound application (1.1 MHz) by cavitation and subsequent Nile Red release	[99]
PEO-b-PNHL	-	Micelle half-life in the systemic circulation can be tailored by composition modifications	[137]

Table III. Ultrasound-Responsive Micelles under clinical trial

Micelle Name	Encapsulated substance	Study type/ Effect	Current Status	Ref.
NK012	SN-38	The encapsulated agents are quickly released from the PEG-PGlu(SN-38) micelles following sonication using HIFU in breast cancer.	Clinical Phase trial II	[138]
Genexol-PM	Paclitaxel	The encapsulated agents are quickly released from the PEG-P(D,L-lactide) micelles following sonication using HIFU in breast, ovarian, pancreatic cancer, and non-small cell lung cancer	Clinical Phase trial I/II	[139]
NK105	Paclitaxel	The encapsulated agents are quickly released from the PEG-P(aspartate) micelles following sonication using HIFU in advanced stomach cancer.	Clinical Phase trial II	[140]–[142]
SP1049C	DOX	The encapsulated agents are quickly released from the Pluronic L61 and F127 micelles following sonication using HIFU in oesophageal adenocarcinoma and stomach cancer cells	Clinical Phase trial III	[143], [144]
NC-6004	Cisplatin	The encapsulated agents are quickly released from the PEG-PGlu (cisplatin) micelles following sonication using HIFU in solid tumors.	Clinical Phase trial I/II	[145], [146]

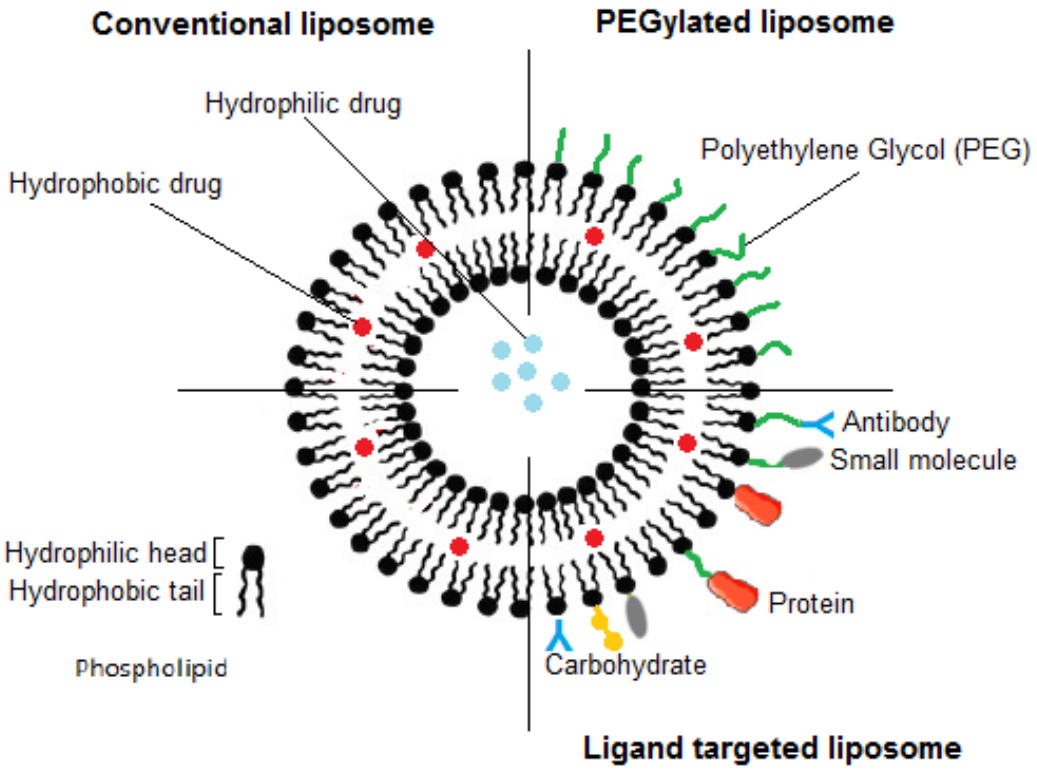

Figure 3. Functionalization of the liposomal surface.

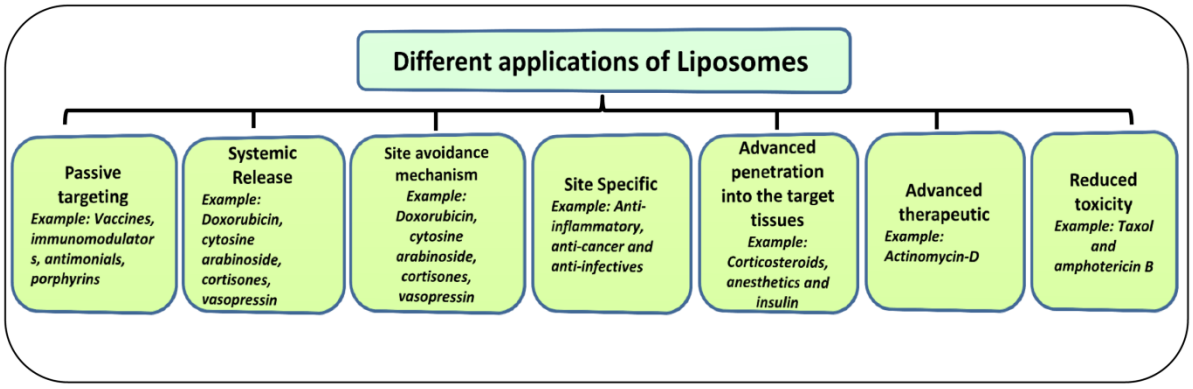

Figure 4. Advantages of liposomal drug delivery.

As mentioned earlier, US waves can trigger liposomal release through localized thermal effects (hyperthermia), or mechanical effects (cavitation of micro-bubbles) (*72*, *73*, *122*). US frequency, pulse duration, and intensity parameters need to be optimized when using US in drug release for treating cancer. The intensity of the US usually varies per application; low-intensity US triggers release from liposomes through mild cavitation and increasing porosity, while high-intensity US triggers release from liposomes due to US-induced hyperthermia and cavitational effects (*29*, *123*, *124*). The presence or formation of microbubbles in liposomes is important towards the success of US in triggering drug release. The interaction of US with liposomes is aided via the presence or the consequential formation of gas micro-bubbles either inside or in close proximity to the liposomes (*74*). To improve the number of cavitation nuclei, emulsions prepared from perfluorocarbons, could be incorporated into the liposome's core or attached/conjugated to its surface (*74*, *125*). These existing or recently formed microbubbles contribute to transient cavitation effects. When these bubbles oscillate with high amplitudes, which exceed their equilibrium radii values, the bubbles expand rapidly then collapse abruptly, generating an instantaneous local rise in pressure and temperature (up to 1000 atm and 5000 K) (*126–128*). In addition, the violent collapse of cavitation bubbles generates microjets traveling at a high velocity, pushing the nearby surfaces and thus enhancing mass transfer or aiding in enhancing the porosity of the nano-vehicles (*129*). Collapse cavitation depends on the type of gas enclosed in the bubble, the size of the bubble, and the US power density and frequency. Low-frequency and high-power density US are favored to generate collapse cavitation. Therefore, for US-mediated drug carriers, acoustic parameters should be optimized for stimulating the drug release while evading detrimental damage to cells and tissues (*74*, *130*). Compared to HFUS (1–3 MHz), LFUS (20–100 kHz) can be a more effective to trigger and sustain release, because it has a deeper penetration capacity into tissues (*41*). The main drawback of using LFUS is that it is difficult to focus on the tumor site.

Acoustically active liposomes, such as bubble liposomes and echogenic liposomes, contain a gaseous phase, which is responsive to ultrasonic waves. These liposomes are prepared by conjugating gas bubbles to the exterior of the liposome. These acoustic bubbles can be activated by applying stress and through ultrasonic cavitation, creating small pores in the liposomal membrane, hence enhancing permeability and enabling the dismantling of the entire liposome (*131*) (*132*). Research has revealed that T-cell dependent tumor growth can be suppressed using bubble liposomes and sonoporation for IL-12 corded plasmid DNA delivery (*133*). However, due to its micron size, echogenic liposomes are favored over bubble liposomes (*134*). Pitt and colleagues (*135–137*) developed emulsion liposomes (eLiposomes) and tested the effects of US on their release. Their studies indicated that by applying US, emulsion droplets would convert from the liquid phase to gaseous phase, rupturing the lipid bilayer of these novel nanocarriers to release their payload (*135–137*). Another category of US-responsive liposomes consists of small liposomes with larger gas bubbles. These liposomes are typically about 100 nm and are loaded with anticancer agents, whereas the bubbles are around1–3 μm and encapsulate a perfluorocarbon gas (*138*, *139*). Upon sonication, the bubble cavitates aggressively, and the subsequent shear waves disrupt nearby vesicles and release the encapsulated contents.

Evjen et al. (*140*) investigated US-sensitive 1,2-dioleoyl-sn-glycero-3-phosphatidylethanolamine (DOPE) liposomes containing DOX. The synthesized liposomes had a size range of 84-88 nm and showed more than 90% Dox release *in vitro*. In 2011 another study by Evjen et al. (*141*) reported a strong association between US sensitivity and non-bilayer forming lipids, as DOPE liposomes showed a higher sonosensitivity and higher stability compared to distearoylphosphatidylethanolamine (DSPE)-based liposomes in the release of calcein. In a study involving eLiposomes, Lattin et al. (*136*) reported that eLiposomes were found to be more effective in killing cancer cells. In a study by Evjen et al. (*142*), liposomes composed of DOPE and hydrogenated soy L-α-phosphatidylcholine (HSPC) demonstrated

high sonosensitivity. Whereas, DOPE-based liposomes had a remarkable change in size and morphology after US, leading to the complete disruption of the liposome and maximum drug release; HSPC liposomes were unaffected in size and structure even after US pore-mediated release. Graham et al. (*143*) showed that liposomes whose formulations contain a high ratio of DSPE released up to 30% of their payload following 0.5-MHz US exposure *in vitro*. Furthermore, in their *in vivo* model, the liposomes showed an almost 16-fold increase in payload release within tumors. Xin et al. (*144*) demonstrated that PLGA NPs prepared using the emulsion solvent evaporation method containing Mitoxantrone (MXT) increased the antitumor efficacy and decreased serious side effects. This system combined the stability of liposomes and the rapid release triggered by HFUS. It exhibited decent stability under test conditions simulating the physiological environment and fast, responsive relief under US. Geers et al. (*145*) showed that liposome-loaded microbubbles were capable of killing human melanoma cells by improved DOX release upon sonication with LFUS. Evjen et al. (*146*) showed that $AlPcS_4$(infrared fluorochrome Al III Phthalocyanine Chloride Tetrasulphonic acid) encapsulated in liposomes was released upon exposure to 1.1-MHz US. The fluorescence levels in prostate cancer xenografted mice increased significantly in the US-treatment group, while no change in fluorescence was in group treated with HSPC-liposomes only. Recently Wrenn et al. (*147*) synthesized SF6 microbubbles, coated with a 95% DSPC/5% DSPE PEG-3000 monolayer, and nested within liposomes. Calcein release was induced using 20-kHz LFUS and was monitored as a function of US pressure. The findings of the study showed that the calcein release occurred with and without the incorporation of microbubbles into the liposomal core. S. Hayashi et al. (*148*) significantly inhibited the tumor growth rate in a metastatic hepatic mouse model treated with liposome-mediated interferon-beta gene therapy combined with US (1MHz). Anwer et al. (*149*) applied US treatment with IL-12 liposomes in SCCVII tumor-bearing mice. The *in vivo* study results showed significantly higher levels of

IL-12 in the tumor and increased inhibition of the tumor growth rate in SCCVII-tumor-bearing mice.

Echogenic immunoliposomes are newly developed nanocarriers combining the advantages of immunoliposomes with the echogenicity or US-responsiveness of microbubbles. Wallace et al. (*147*) synthesized echogenic immunoliposomes by conjugating echogenic liposomes with bevacizumab, a tumor-targeting antibody. The developed liposomes showed high bevacizumab penetration in *ex vivo* carotid arteries when treated with BEV-ELIP and color-Doppler US. Klegerman et al. (*150*) extended the aforementioned experiment to human umbilical vein endothelial cell (HUVEC) cultures. A study by Zolochevska et al. (*151*) utilized US and microbubble enhanced cytokine (pORF-mIL-27) delivery for the treatment of prostate cancer. The developed system resulted in a reduction of prostate tumor in murine prostate cancer cell lines, TRAMP-C1 and TRAMP-C2. Oda et al. (*152*) investigated a melanoma-derived antigen delivered using microbubbles and US. Their findings showed a decreased melanoma lung metastasis frequency in the B16/BL6 melanoma cell line and lung metastasis mouse model. Shi et al. (*153*) utilized microbubbles and US to deliver regulatory T cells (Foxp3-miRNA/shRNA) to patients with HCC, resulting in a decreased ratio of regulatory T cells and CD4+ T cells and suppressed tumor growth. The same group used SonoVue® microbubbles and US to deliver CCD4+CD25+ regulatory T cells (Tregs) in hepatocellular carcinomas, which resulted in increased Tregs proliferation (*154*). Definity® liposomes, consisting of NK cells (NK-92), were used in conjunction with focused US to treat human HER2-expressing MDA-mB-231 breast tumor cells (*155*). The study resulted in HER2-specific NK92 cells accumulating at the tumor site, suppressed tumor growth, and increased survival. Maria et al. (*156*) treated human colorectal adenocarcinoma cells (LS174T) with microbubbles, NK cells, and US; resulting in NK cell accumulation in tumors and increased water content and edema. Heath et al. (*157*) used microbubbles with the tumor-targeting antibody, cetuximab, to treat

human head and neck squamous carcinoma cell lines in 6-week old xenograft mice inoculated with BT474. The *in vivo* results showed suppressed tumor growth and increased survival when applied with ultrasound. Similarly, in a study by Park et al. (*158*), microbubble and US-mediated treatment with trastuzumab resulted in suppressed tumor growth and increased survival in HER2/neu-positive human breast cancer cells BT575 and 6-week old xenograft mice inoculated with BT474. Table IV presents a summary of several recent studies on US-sensitive liposomes.

2. Conclusion

The aim of efficient nanocarrier-based drug delivery systems is to achieve therapeutic concentration of anticancer drugs while using lower systemic chemotherapeutic drug dosages. This in turn would reduce the costs and alleviate some of the adverse side effects associated with chemotherapy. . Nanocarrier properties (such as the size, shape, material substrate, and surface chemistry) play a vital role in the therapeutic efficacy of developed system. Liposomes and micelles are two of the most widely employed nanocarriers in drug delivery applications. In addition, the modification of micellar and liposomal surfaces with targeting moieties and the use of a triggering mechanism, such as US, can greatly help improve the selectivity and enable the control of the temporal and spatial drug release from these nanocarriers. However, further research is still needed to develop a deeper understanding of the interactions occurring in diseased tissues. Such knowledge is fundamental to develop efficient smart nanocarriers. In this review, we highlighted recent advancements in the development of smart nanocarriers, focusing on US-triggered release from micelles and liposomes.

Conflicts of Interest

The authors declare that there is no conflict of interest regarding the publication of this paper.

Acknowledgments

The authors would like to acknowledge funding from AUS Faculty Research Grants, Patient's Friends Committee-Sharjah, AlJalila Foundation, Al Qasimi Foundation, the Technology Innovation Pioneer-Healthcare Program, the Takamul program, and the Dana Gas Endowed Chair for Chemical Engineering.

Table IV. Examples of recent studies on ultrasound-sensitive liposomes

Liposome Constituents	Encapsulated substance	US parameters	In vitro study	In vivo study	Overview	Ref.
DOPE	DOX	40 kHz for 6 min	-	-	• US-sensitive DOPE liposomes containing DOX were able to release more than 90% of their encapsulated contents *in vitro*.	[165]
DSPC, Chol, DSPE-PEG, DOPE	Calcein	1.13 MHz	-		• Calcein was released from DOPE-based liposomes. • Non-bilayer forming lipids DOPE and DSPE-PEG 2000 showed more stability compare to DSPE-based liposomes in terms of calcein release.	[166]
DPPC liposome with internal emulsion droplets	Marker as an emulsion droplet	20 kHz	-	-	• Emulsion droplets were formed from PFC6 by sonication at 20 kHz and stabilized with DPPC.	[161]
DOPE and HSPC	DOX	40 kHz	-	-	• DOPE liposomes showed a remarkable change in their size and morphology after US. • HSPC liposomes persisted unaffected in size and structure even after US-mediated release.	[167]
DSPC, Chol, DSPE-PEG, DOPE	Infrared fluorochrome Al (III) Phthalocyanine Chloride Tetrasulphonic acid ($AlPcS_4$)	1.1. MHz	Prostate tumor cells 22Rv1	Xenograft mice inoculated with prostate cancer cells	• Encapsulated $AlPcS_4$ was released upon 1.1-MHz US exposure resulted in a significant increase in fluorescence in mice treated with free $AlPcS_4$ but no change in the mice treated with HSPC-based liposomes.	[171]
HSPC, Chol, DSPE, DSPE-PEG	DOX & marker	-	Metastatic murine melanoma (B16F10 luciferase cells)	-	• Liposomes formulated with a high proportion of DSPE released up to 30% of payload following 0.5-MHz ultrasound exposure *in vitro* and a 16-fold increase in the level of payload release *in vivo*.	[168]
PLGA NPs: HSPC, Chol, DSPE-PEG2000 and DSPC	Mitoxantrone (MXT)	HIFU (> 1 MHz)	-	Adult Sprague-Dawley rats	• PLGA NPs exhibited decent stability under physiological conditions and fast responsive relief under US.	[169]
liposome-loaded (lipid-shelled) microbubbles	DOX	1 MHz	Human melanoma BLM cells	-	• Liposome-loaded microbubbles were thoroughly characterized and proven capable of killing cancer cells by improved DOX release upon exposure to LFUS	[170]
DPPC, Chol, DSPE-PEG, PDP, DOPE	Marker: indocyanine green (ICG)	1MHz	-	Female NMRI mice	• Results confirmed ICG deposition which was almost double in microbubble loaded mice compared to control mice.	[164]
DSPC, DSPE-PEG	IL-12 corded pDNA	1MHz	Murine ovarian carcinoma (OV-HM cells)	-	• Combination of 1 MHz ultrasound and bubble liposomes resulted in significant migration of CD8(+) T cells in mice.	[158]

Liposome Constituents	Encapsulated substance	US parameters	In vitro study	In vivo study	Overview	Ref.
microbubbles	NK cells	510 kHz transducer,0.50 MPa peak acoustic pressure	Human colorectal adenocarcinoma cells (LS174T)	-	• NK cell accumulation in tumors increased water content and edema.	[181]
Emtansine (DM1) microbubbles	Trastuzumab and Pertuzumab	FUS 10-ms bursts, 1 Hz repetition frequency, 60 s duration. Acoustic powers of 0.4-0.7 W	MDA MB-361 cells	-	• BBB disruption using FUS in combination with antibody therapy inhibited the growth of breast cancer brain metastasis.	[184]
microbubble	Cetuximab	1 MHz, MI: 0.5, a pulse repetition period of 5s, 20% duty cycle, 5 min	Human head and neck squamous carcinoma cell lines	6-week old xenograft mice inoculated with BT474	• Suppressed tumor growth and increased survival.	[182]
microbubbles	Tumor targeting antibody (Trastuzumab)	PRF:1 Hz, 1% DC, PNP:0.69 MPa, sonications were 60 s in duration and 10 m bursts	HER2/neu-positive human breast cancer cells BT474	6-week old xenograft mice inoculated with BT474	• Suppressed tumor growth and increased survival	[183]
microbubbles	Anti PD-1 antibody	1 MHz, 50 0.1-ms-long pulses spaced 1m apart, 20 s intervals, duration of 2 min Peak negative pressures 1.65 MPa	Murine colorectal cancer cell line CT26	-	• Suppressed tumor growth and increased survival.	[185]
PC, Chol, PEG150 stearate, Biotin-PEG3400-PC	Thrombin, Marker	1MHz	-	-	• More than 30% thrombin and calcein were released from biotinylated decafluorobutane microbubbles upon exposure to US at a frequency of 1MHz.	[163]
SF6 microbubbles coated by a 95% DSPC/5% DSPE PEG-3000 monolayer	Calcein	20 kHz	-	-	• Release occurred using 20-kHz LFUS with and without microbubbles incorporated into the liposome core. • Complete membrane damage was observed for samples exposed to HFUS at more than 1 MHz.	[172]
11In-EGF-LP	DOX	1.1 MHz	Breast cancer cell lines MDA-MB-468 & MCF7.	MDA-MB-468 Female xenografts	• Delivery to tumors was enhanced using US-mediated cavitation.	[186]

Liposome Constituents	Encapsulated substance	US parameters	In vitro study	In vivo study	Overview	Ref.
Liposome	Gadolinium and rhodamine	1.1 MHz	-	Male mice	• Dual- labeled nanocarrier platform can be established, the FUS-mediated BBB opening approach can be used to deliver it through vascular barriers, and MRI can be used to evaluate the extent of nanocarrier delivery.	[187]
Liposome	Cytokine (IFNbeta)	1 MHz, 0.5 W/cm^2, 20% duty cycle, 30 s; *in vivo*:1 MHz, 2 W/cm^2, 50% duty cycle, 10 min;	Murine colon adenocarcinoma cell line Colo 26	Xenograft mice model inoculated with Colo26	• Suppressed tumor growth and increased survival	[173]
Liposome	Cytokine (IL-12)	1 MHz, 0.7 W/cm^2, 60s	Squamous carcinoma cells	6–8-week-old female SCCVII-tumor-bearing mice	• Ultrasound treatment produced significantly higher levels of IL-12 in tumors, that further inhibit tumor growth compared with the control conditions.	[174]
Liposome	Tumor targeting antibody (Trastuzumab)	20kHz, 7.46-17.31 mW/cm2	HER2-positive breast cancer	-	• Enhanced release rates.	[188]
Echogenic immunoliposomes	Anti-smooth muscle cell actin antibody	1 MHz, 0.23 ± 0.05 MPa, 2 min	Vascular smooth muscle cells	-	• Increased site-specific calcein uptake.	[189]
Echogenic immunoliposomes	Tumor targeting antibody (bevacizumab)	Scanned-mode pulsed Doppler ultrasound (1.75 MHz center frequency and 10 cycle pulse duration)	Ex vivo carotid arteries	-	• Strong bevacizumab penetration, was observed in arteries treated with BEV-ELIP and combinations of color-Doppler US, especially in arteries exhibiting extensive atheromatous lesions and neointima.	[190]
Echogenic immunoliposomes	Tumor targeting antibody (bevacizumab)	6 MHz color Doppler ultrasound (MI = 0.4) for 5 min.	Human umbilical vein endothelial cell (HUVEC) cultures	-	• Doppler US significantly increased the VEGF-binding activity, both by releasing free BEV and by enhancing the surface exposure of the immunoreactive antibody.	[175]
Microbubble	Cytokine (pORF-mIL-27)	1 MHz, 50% duty cycle, 45 V, 2 Hz, 2 min, 1 W/cm^2, acoustic pressure of 0.12 MPa	Murine prostate cancer cell line TRAMP-C1 and TRAMP-C2	-	• Reduction in the size of prostate tumors	[176]

Liposome Constituents	Encapsulated substance	US parameters	In vitro study	In vivo study	Overview	Ref.
Man-PEG$_{2000}$ bubble lipoplexes	Dendritic cell Vaccine (pDNA expresses OVA)	2.062 MHz, duty cycle 50%; burst rate, 10 Hz; 4.0 W/cm^2, 20 s	CD8-OVA1.3 cells, EL4 cells, E.G7-OVA	-	• Suppressed tumor growth.	[191]
Man-PEG$_{2000}$ bubble lipoplexes	Dendritic cell Vaccine (pDNA expresses gp100 and TRP-2)	1.045 MHz; duty, 50%; burst rate, 10 Hz; 1.0 W/cm^2; 2 min	B16BL6 melanoma cells	-	• Increased CTLs prevented metastasis and relapsed melanoma.	[192]
microbubble	Dendritic cell Vaccine (Melanoma-derived antigen)	2 MHz, 2 W/cm2, 10% duty, 3x10 seconds	B16/BL6 melanoma cell line	Mouse model with lung metastasis	• A decrease in the frequency of melanoma lung metastasis.	[177]
mRNA-lipoplex loaded microbubbles	Dendritic cell Vaccine (mRNA)	1 MHz, 2 W/cm^2, 50% duty cycle, 30 s	-	DC from bone marrow of C57Bl/6 mice	• DC maturation.	[193]
mRNA-loaded microbubbles	Dendritic cell Vaccine (antigen mRNA and TriMix mRNA)	1 MHz, 2 W/cm^2, peak-negative pressure 800 kPa, 20% duty cycle (2 m on, 8 m off), 30 s total insonation time per OptiCell™	Mouse melanoma cell line MO4 and T cell lymphoma E.G7-OVA	Mice with OVA tumors	• Increased CD8 + T cells, which suppressed tumor growth and increased survival.	[194]
microbubbles	Regulatory T cells (Foxp3-miRNA/shRNA)	2.5 MHz, MI of 1.4, 150/181 s	Tregs from patients with HCC	-	• Decreased ratio of Tregs/CD4+ T cells suppressed tumor growth.	[178]
SonoVue ® microbubble	CCD4+CD25+ regulatory T cells (Tregs)	1.4 MI, 150 or 180 sec	Hepatocellular carcinoma	-	• Increased Treg proliferation.	[179]
Definity®	NK cells (NK-92)	551.5 kHz focused ultrasound transducer, range 0.32–0.35 MPa	Human HER2-expressing MDA-MB-231 breast tumor cells	-	HER2-specific NK92 cells accumulating in tumors suppressed tumor growth and increased survival	[175]–[178], [184]–[187]

Abbreviations: Chol: Cholesterol; DLPA: 1,2-Didodecanoyl-snglycero-3-phosphate (sodium salt); DMPC: 1,2-Dimyristoyl-sn-glycero-3-phosphocholine; DOPE: 1,2-Dioleoylsn-glycero-3-phosphoethanolamine; DOX: Doxorubicin; DPPA: 1,2-Dipalmitoyl-sn-glycero-3-phosphate; DPPC: 1,2-Dipalmitoyl-sn-glycero-3-phosphocholine; DSPC: 1,2-Distearoyl-sn-glycero-3-phosphocholine; DSPE: 1,2-Distearoyl-sn-glycero-3-phosphoethanolamine; DSPE-PEG: 1,2-Distearoyl-sn-glycero-3-phosphoethanolamine-(polyethylene glycol)-2000; DSPE-PEG-SPDP: 1,2-Distearoyl-sn-glycero-3-phosphoethanolamine-[N-PDP(polyethylene glycol)-2000]; HSPC: Hydrogenated soy phosphocholine; PC: Phosphatidylcholine; pDNA: Plasmid DNA; PDP: 3-(2-Pyridyldithio)-Propionate; POPC: 1-Palmitoy L-2-oleoyl-sn-glycero-3-phosphocholine; PCF6: Perfluorohexane.

References

1. Breast Cancer Research Articles - National Cancer Institute.

2. G. M. Cooper, (2000).

3. M. Arruebo *et al.*, Assessment of the evolution of cancer treatment therapies. *Cancers (Basel).* **3** (2011), pp. 3279–3330.

4. C.-Y. Huang, D.-T. Ju, C.-F. Chang, P. M. Reddy, B. K. Velmurugan, *BioMedicine*. **7**, 23 (2017).

5. K. M. Islam *et al.*, *BMC Cancer*. **19**, 835 (2019).

6. H. M. Buiting *et al.*, *PLoS One*. **8**, e77959 (2013).

7. P. S. Rajagopal, R. D. Nipp, K. J. Selvaggi, *Ann. Palliat. Med.* **3**, 203–20328 (2014).

8. D. Abbott *et al.*, *F1000Research*. **4**, 1 (2015).

9. S. E. Harrington, T. J. Smith, The role of chemotherapy at the end of life: "When is enough, enough?" *JAMA - J. Am. Med. Assoc.* **299** (2008), pp. 2667–2678.

10. V. T. DeVita, E. Chu, *Cancer Res.* **68**, 8643–8653 (2008).

11. American Cancer Society, Evolution of Cancer Treatments: Chemotherapy (2014), (available at https://www.cancer.org/cancer/cancer-basics/history-of-cancer/cancer-treatment-chemo.html).

12. E. J. Devlin, L. A. Denson, H. S. Whitford, Cancer Treatment Side Effects: A Meta-analysis of the Relationship Between Response Expectancies and Experience. *J. Pain Symptom Manage.* **54** (2017), pp. 245-258.e2.

13. A. Pearce *et al.*, *PLoS One*. **12** (2017), doi:10.1371/journal.pone.0184360.

14. L. Y. Ramirez *et al.*, *Pediatr. Blood Cancer*. **52**, 497–502 (2009).

15. K. Nurgali, R. T. Jagoe, R. Abalo, Editorial: Adverse effects of cancer chemotherapy: Anything new to improve tolerance and reduce sequelae? *Front. Pharmacol.* **9** (2018), , doi:10.3389/fphar.2018.00245.

16. E. S. Kawasaki, A. Player, Nanotechnology, nanomedicine, and the development of new, effective therapies for cancer. *Nanomedicine Nanotechnology, Biol. Med.* **1** (2005), pp. 101–109.

17. Y. Hong, Y. Rao, Current status of nanoscale drug delivery systems for colorectal cancer liver metastasis. *Biomed. Pharmacother.* **114** (2019), p. 108764.

18. D. Liu, F. Yang, F. Xiong, N. Gu, The smart drug delivery system and its clinical potential. *Theranostics*. **6** (2016), pp. 1306–1323.

19. F. U. Din *et al.*, *Int. J. Nanomedicine*. **12**, 7291–7309 (2017).

20. J. K. Patra *et al.*, *J. Nanobiotechnology*. **16** (2018), doi:10.1186/s12951-018-0392-8.

21. S. Senapati, A. K. Mahanta, S. Kumar, P. Maiti, Controlled drug delivery vehicles for cancer treatment and their performance. *Signal Transduct. Target. Ther.* **3** (2018), , doi:10.1038/s41392-017-0004-3.

22. A. Wicki, D. Witzigmann, V. Balasubramanian, J. Huwyler, Nanomedicine in cancer therapy: Challenges, opportunities, and clinical applications. *J. Control. Release*. **200** (2015), pp. 138–157.

23. M. W. Kim, S. H. Kwon, J. H. Choi, A. Lee, A promising biocompatible platform: Lipid-based and bio-inspired smart drug delivery systems for cancer therapy. *Int. J. Mol. Sci.* **19** (2018), , doi:10.3390/ijms19123859.

24. G. Bozzuto, A. Molinari, Liposomes as nanomedical devices. *Int. J. Nanomedicine*. **10** (2015), pp. 975–999.

25. W. Gao, C. M. J. Hu, R. H. Fang, L. Zhang, *J. Mater. Chem. B*. **1**, 6569–6585 (2013).

26. N. M. Al Sawaftah, G. A. Husseini, *J. Nanosci. Nanotechnol.* **20**, doi:10.1166/jnn.2020.18877.

27. S. E. Ahmed, N. Awad, V. Paul, H. G. Moussa, G. A. Husseini, *Curr. Top. Med. Chem.* **18**, 857–880 (2018).

28. W. G. Pitt, *Am. J. Drug Deliv.* **1**, 27–42 (2003).

29. W. G. Pitt, G. Husseini, B. J. Staples, Ultrasonic drug delivery - A general review. *Expert Opin. Drug Deliv.* **1** (2004), pp. 37–56.

30. Y. D. Livney, Y. G. Assaraf, *Adv. Drug Deliv. Rev.* **65**, 1716–1730 (2013).

31. A. Schroeder, J. Kost, Y. Barenholz, *Chem. Phys. Lipids*. **162**, 1–16 (2009).

32. T. J. Mason, in *Ultrasonics Sonochemistry* (Elsevier B.V., 2011), vol. 18, pp. 847–852.

33. Q. Ye *et al.*, Reversal of multidrug resistance in cancer by multi-functional flavonoids. *Front. Oncol.* **9** (2019), p. 487.

34. F. Wu, Z. Y. Shao, B. J. Zhai, C. L. Zhao, D. M. Shen, *Ultrasound Med. Biol.* **37**, 151–159 (2011).

35. Z. QL *et al.*, *Biomed Res. Int.* **2014** (2014), doi:10.1155/2014/963891.

36. S. Wilhelm *et al.*, Analysis of nanoparticle delivery to tumours. *Nat. Rev. Mater.* **1** (2016), pp. 1–12.

37. J. Wang, M. Pelletier, H. Zhang, H. Xia, Y. Zhao, *Langmuir*. **25**, 13201–13205 (2009).

38. S. Raj *et al.*, Specific targeting cancer cells with nanoparticles and drug delivery in cancer therapy. *Semin. Cancer Biol.* (2019), , doi:10.1016/j.semcancer.2019.11.002.

39. W. M. Saltzman, V. P. Torchilin, *Access Sci.* (2018), doi:10.1036/1097-8542.757275.

40. M. Mahmoud, thesis, American University of Sharjah (2018).

41. Smart Pharmaceutical Nanocarriers - Google Books.

42. N. T. T. Le *et al.*, Recent progress and advances of multi-stimuli-responsive dendrimers in drug delivery for cancer treatment. *Pharmaceutics*. **11** (2019), , doi:10.3390/pharmaceutics11110591.

43. B. Huang *et al.*, *Drug Des. Devel. Ther.* **9**, 3867–3876 (2015).

44. J. Manikkath, A. Manikkath, G. V. Shavi, K. Bhat, S. Mutalik, *J. Drug Deliv. Sci. Technol.* **41**, 334–343 (2017).

45. R. Arvizo, R. Bhattacharya, P. Mukherjee, Gold nanoparticles: Opportunities and challenges in nanomedicine. *Expert Opin. Drug Deliv.* **7** (2010), pp. 753–763.

46. S. T. Kang, Y. L. Luo, Y. F. Huang, C. K. Yeh, in *IEEE International Ultrasonics Symposium, IUS* (2012), pp. 1866–1868.

47. C. Brazzale *et al.*, *Nanomedicine*. **11**, 3053–3070 (2016).

48. M. Ibrahim, R. Sabouni, G. A. Husseini, *J. Nanosci. Nanotechnol.* **18**, 5266–5273 (2018).

49. X. Pan *et al.*, *Adv. Mater.* **30** (2018), doi:10.1002/adma.201800180.

50. T.-Y. Wang, K. Wilson, S. Machtaler, J. Willmann, *Curr. Pharm. Biotechnol.* **14**, 743–752 (2014).

51. L. H. Treat, N. McDannold, Y. Zhang, N. Vykhodtseva, K. Hynynen, *Ultrasound Med. Biol.* **38**, 1716–1725 (2012).

52. C. Y. Ting *et al.*, *Biomaterials*. **33**, 704–712 (2012).

53. V. P. Torchilin, *Cell. Mol. Life Sci.* **61**, 2549–59 (2004).

54. V. P. Torchilin, Micellar nanocarriers: Pharmaceutical perspectives. *Pharm. Res.* **24** (2007), pp. 1–16.

55. M. C. I. M. Amin, A. M. Butt, M. W. Amjad, P. Kesharwani, in *Nanotechnology-Based Approaches for Targeting and Delivery of Drugs and Genes* (Elsevier Inc., 2017), pp. 167–202.

56. Y. Lu, E. Zhang, J. Yang, Z. Cao, Strategies to improve micelle stability for drug delivery. *Nano Res.* **11** (2018), pp. 4985–4998.

57. N. A. N. Hanafy, M. El-Kemary, S. Leporatti, Micelles structure development as a strategy to improve smart cancer therapy. *Cancers (Basel).* **10** (2018), , doi:10.3390/cancers10070238.

58. G. Kwon *et al.*, *Langmuir*. **9**, 945–949 (1993).

59. G. S. Kwon, K. Kataoka, Block copolymer micelles as long-circulating drug vehicles. *Adv. Drug Deliv. Rev.* **16** (1995), pp. 295–309.

60. G. Kwon *et al.*, *J. Control. Release*. **48**, 195–201 (1997).

61. K. Kazunori, K. Glenn S., Y. Masayuki, O. Teruo, S. Yasuhisa, *J. Control. Release*. **24**, 119–132 (1993).

62. E. Batrakova *et al.*, *Pharm. Res.* **16**, 1373–1379 (1999).

63. G. A. Husseini, W. G. Pitt, *J. Nanosci. Nanotechnol.* **8**, 2205–2215 (2008).

64. J. Dai *et al.*, *Signal Transduct. Target. Ther.* **5**, 145 (2020).

65. D. Ha, N. Yang, V. Nadithe, Exosomes as therapeutic drug carriers and delivery vehicles across biological membranes: current perspectives and future challenges. *Acta Pharm. Sin. B*. **6** (2016), pp. 287–296.

66. E. J. Bunggulawa *et al.*, Recent advancements in the use of exosomes as drug delivery systems 06 Biological Sciences 0601 Biochemistry and Cell Biology. *J. Nanobiotechnology*. **16** (2018), p. 81.

67. W. Sun, Z. Li, X. Zhou, G. Yang, L. Yuan, *Drug Deliv.* **26**, 45–50 (2019).

68. Y. Liu *et al.*, *Theranostics*. **9**, 5261–5281 (2019).

69. H. Xia, Y. Zhao, R. Tong, Ultrasound-mediated polymeric micelle drug delivery. *Adv. Exp. Med. Biol.* **880** (2016), pp. 365–384.

70. N. Rapoport, *Int. J. Hyperth.* **28**, 374–385 (2012).

71. G. A. Husseini, R. I. El-Fayoumi, K. L. O'Neill, N. Y. Rapoport, W. G. Pitt, *Cancer Lett.* **154**, 211–216 (2000).

72. G. A. Husseini, M. A. Diaz De La Rosa, E. S. Richardson, D. A. Christensen, W. G. Pitt, *J. Control. Release*. **107**, 253–261 (2005).

73. G. A. Husseini, G. D. Myrup, W. G. Pitt, D. A. Christensen, N. Y. Rapoport, *J. Control. Release*. **69**, 43–52 (2000).

74. G. A. Husseini, W. G. Pitt, A. M. Martins, *Colloids Surfaces B Biointerfaces*. **123**, 364–386 (2014).

75. N. Munshi, N. Rapoport, W. G. Pitt, *Cancer Lett.* **118**, 13–9 (1997).

76. G. A. Husseini *et al.*, *Colloids Surf. B. Biointerfaces*. **101**, 153–5 (2013).

77. G. A. Husseini, W. G. Pitt, Micelles and nanoparticles for ultrasonic drug and gene delivery. *Adv. Drug Deliv. Rev.* **60** (2008), pp. 1137–1152.

78. N. Y. Rapoport, J. N. Herron, W. G. Pitt, L. Pitina, *J. Control. Release*. **58**, 153–162 (1999).

79. A. Marin, M. Muniruzzaman, N. Rapoport, *J. Control. Release*. **71**, 239–249 (2001).

80. A. Marin, M. Muniruzzaman, N. Rapoport, *J. Control. Release*. **75**, 69–81 (2001).

81. A. Marin *et al.*, *J. Control. Release*. **84**, 39–47 (2002).

82. G. A. Husseini, D. A. Christensen, N. Y. Rapoport, W. G. Pitt, *J. Control. Release*. **83**, 303–305 (2002).

83. M. A. Diaz de la Rosa, thesis, Brigham Young University (2007).

84. D. Kobayashi, M. Karasawa, T. Takahashi, K. Otake, A. Shono, in *Japanese Journal of Applied Physics* (2012), vol. 51.

85. G. A. Husseini *et al.*, *Colloids Surfaces A Physicochem. Eng. Asp.* **359**, 18–24 (2010).

86. D. Stevenson-Abouelnasr, G. A. Husseini, W. G. Pitt, *Colloids Surfaces B Biointerfaces*. **55**, 59–66 (2007).

87. B. J. Staples *et al.*, *Cancer Chemother. Pharmacol.* **64**, 593–600 (2009).

88. N. Rapoport, *Colloids Surfaces B Biointerfaces*. **16**, 93–111 (1999).

89. G. A. Husseini, N. Y. Rapoport, D. A. Christensen, J. D. Pruitt, W. G. Pitt, *Colloids Surfaces B Biointerfaces*. **24**, 253–264 (2002).

90. G. A. Husseini *et al.*, *J. Nanosci. Nanotechnol.* **7**, 1028–33 (2007).

91. Y. Zeng, W. G. Pitt, *J. Biomater. Sci. Polym. Ed.* **17**, 591–604 (2006).

92. G. A. Husseini, W. G. Pitt, D. A. Christensen, D. J. Dickinson, *J. Control. Release*. **138**, 45–48 (2009).

93. G. A. Husseini *et al.*, *Colloids Surfaces B Biointerfaces*. **101**, 153–155 (2013).

94. Y. Chen *et al.*, *Int. J. Nanomedicine*. **8**, 1463–1476 (2013).

95. P. Wu *et al.*, *ACS Appl. Mater. Interfaces*. **9**, 25706–25716 (2017).

96. M. Maeda *et al.*, *Ultrasound Med. Biol.* **43**, 2295–2301 (2017).

97. Y. Horise *et al.*, *Front. Pharmacol.* **10**, 545 (2019).

98. K. Takemae, J. Okamoto, Y. Horise, K. Masamune, Y. Muragaki, *Front. Pharmacol.* **10**, 546 (2019).

99. H. Zhang, H. Xia, J. Wang, Y. Li, *J. Control. Release*. **139**, 31–9 (2009).

100. Y. Li, R. Tong, H. Xia, H. Zhang, J. Xuan, *Chem. Commun.* **46**, 7739–7741 (2010).

101. P. Tharkar, R. Varanasi, W. S. F. Wong, C. T. Jin, W. Chrzanowski, Nano-Enhanced Drug Delivery and Therapeutic Ultrasound for Cancer Treatment and Beyond. *Front. Bioeng. Biotechnol.* **7** (2019), p. 324.

102. S. S. Daoud, L. R. Hume, R. L. Juliano, *Adv. Drug Deliv. Rev.* **3**, 405–418 (1989).

103. P. P. Deshpande, S. Biswas, V. P. Torchilin, Current trends in the use of liposomes for tumor targeting. *Nanomedicine*. **8** (2013), pp. 1509–1528.

104. N. Monteiro, A. Martins, R. L. Reis, N. M. Neves, Liposomes in tissue engineering and regenerative medicine. *J. R. Soc. Interface*. **11** (2014), , doi:10.1098/rsif.2014.0459.

105. A. Salimi, *Asian J. Pharm. Free full text Artic. from Asian J Pharm*. **12** (2018), doi:10.22377/AJP.V12I01.2037.

106. A. Akbarzadeh *et al.*, *Nanoscale Res. Lett.* **8**, 102 (2013).

107. Unilamellar Liposome - an overview | ScienceDirect Topics.

108. Preparing Large, Unilamellar Vesicles by Extrusion (LUVET) | Avanti Polar Lipids.

109. C. Dwivedi, S. Verma, *J. Sci. Innov. Res.* **2**.

110. P. N. Shek, B. Y. Yung, N. Z. Stanacev, *Immunology*. **49**, 37–44 (1983).

111. S. M. Gruner, R. P. Lenk, A. S. Janoff, M. J. Ostro, *Biochemistry*. **24**, 2833–2842 (1985).

112. Mempro™ Multivesicular Vesicles Liposomes - Creative Biostructure.

113. H. Mu *et al.*, *Drug Deliv.* **25**, 1372–1383 (2018).

114. T. Wang, L. Gao, D. Quan, *J. Pharm. Pharmacol.* **63**, 904–910 (2011).

115. M. Çağdaş, A. D. Sezer, S. Bucak, in *Application of Nanotechnology in Drug Delivery* (InTech, 2014).

116. K. W. Ferrara, Driving delivery vehicles with ultrasound. *Adv. Drug Deliv. Rev.* **60** (2008), pp. 1097–1102.

117. L. Sercombe *et al.*, Advances and challenges of liposome assisted drug delivery. *Front. Pharmacol.* **6** (2015), , doi:10.3389/fphar.2015.00286.

118. D. C. Litzinger, A. M. J. Buiting, N. van Rooijen, L. Huang, *BBA - Biomembr.* **1190**, 99–107 (1994).

119. J. S. Suk, Q. Xu, N. Kim, J. Hanes, L. M. Ensign, PEGylation as a strategy for improving nanoparticle-based drug and gene delivery. *Adv. Drug Deliv. Rev.* **99** (2016), pp. 28–51.

120. H. Xing, K. Hwang, Y. Lu, Recent developments of liposomes as nanocarriers for theranostic applications. *Theranostics*. **6** (2016), pp. 1336–1352.

121. R. R. Sawant, V. P. Torchilin, Challenges in development of targeted liposomal therapeutics. *AAPS J.* **14** (2012), pp. 303–315.

122. K. Greish, T. Sawa, J. Fang, T. Akaike, H. Maeda, *J. Control. Release*. **97**, 219–230 (2004).

123. A. Sadeghi-Naini *et al.*, *Transl. Oncol.* **6**, 234–243 (2013).

124. D. R. Mittelstein *et al.*, *Appl. Phys. Lett.* **116** (2020), doi:10.1063/1.5128627.

125. J. R. Lattin, W. G. Pitt, D. M. Belnap, G. A. Husseini, *Ultrasound Med. Biol.* **38**, 2163–2173 (2012).

126. The Acoustic Bubble - T. G. Leighton - Google Books.

127. A. E. Catania, A. Ferrari, M. Manno, E. Spessa, *J. Eng. Gas Turbines Power*. **128**, 434–445 (2006).

128. W. B. McNamara, Y. T. Didenko, K. S. Suslick, *Nature*. **401**, 772–775 (1999).

129. M. Keswani, S. Raghavan, P. Deymier, in *Microelectronic Engineering* (Elsevier, 2013), vol. 102, pp. 91–97.

130. S. E. Ahmed, A. M. Martins, G. A. Husseini, The use of ultrasound to release chemotherapeutic drugs from micelles and liposomes. *J. Drug Target.* **23** (2015), pp. 16–42.

131. S. Ibsen *et al.*, *J. Control. Release*. **155**, 358–366 (2011).

132. M. F. Chung *et al.*, *Angew. Chemie - Int. Ed.* **51**, 10089–10093 (2012).

133. R. Suzuki *et al.*, *J. Control. Release*. **142**, 245–250 (2010).

134. Y. Negishi *et al.*, *J. Control. Release*. **132**, 124–130 (2008).

135. C.-Y. Lin, M. Javadi, D. M. Belnap, J. R. Barrow, W. G. Pitt, *Nanomedicine Nanotechnology, Biol. Med.* **10**, 67–76 (2014).

136. J. R. Lattin, D. M. Belnap, W. G. Pitt, *Colloids Surfaces B Biointerfaces*. **89**, 93–100 (2012).

137. M. Javadi, W. G. Pitt, D. M. Belnap, N. H. Tsosie, J. M. Hartley, *Langmuir*. **28**, 14720–14729 (2012).

138. A. L. Klibanov, T. I. Shevchenko, B. I. Raju, R. Seip, C. T. Chin, *J. Control. Release*. **148**, 13–17 (2010).

139. S. K. Cool *et al.*, *J. Control. Release*. **172**, 885–893 (2013).

140. T. J. Evjen *et al.*, *Eur. J. Pharm. Sci.* **42**, 380–386 (2011).

141. T. J. Evjen *et al.*, *Int. J. Pharm.* **406**, 114–116 (2011).

142. T. J. Evjen *et al.*, *J. Pharm. Biomed. Anal.* **78**–**79**, 118–22 (2013).

143. S. M. Graham *et al.*, *J. Control. Release*. **178**, 101–107 (2014).

144. Y. Xin, Q. Qi, Z. Mao, X. Zhan, *Int. J. Pharm.* **528**, 47–54 (2017).

145. B. Geers *et al.*, *J. Control. Release*. **152**, 249–256 (2011).

146. T. J. Evjen *et al.*, *Eur. J. Pharm. Biopharm.* **84**, 526–531 (2013).

147. N. Wallace, S. P. Wrenn, *Ultrasonics*. **63**, 31–38 (2015).

148. S. Hayashi, M. Mizuno, J. Yoshida, A. Nakao, *Cancer Gene Ther.* **16**, 638–643 (2009).

149. K. Anwer *et al.*, *Gene Ther.* **7**, 1833–1839 (2000).

150. M. E. Klegerman *et al.*, *J. Liposome Res.* **26**, 47–56 (2016).

151. O. Zolochevska *et al.*, *Hum. Gene Ther.* **22**, 1537–1550 (2011).

152. Y. Oda *et al.*, *J. Control. Release*. **160**, 362–366 (2012).

153. C. Shi *et al.*, *Exp. Ther. Med.* **15**, 31–38 (2018).

154. C. Shi *et al.*, *Ultrasonics*. **62**, 97–102 (2015).

155. R. Alkins, A. Burgess, R. Kerbel, W. S. Wels, K. Hynynen, *Neuro. Oncol.* **18**, 974–981 (2016).

156. N. S. S. Maria *et al.*, *PLoS One*. **10** (2015), doi:10.1371/journal.pone.0142767.

157. C. H. Heath, A. Sorace, J. Knowles, E. Rosenthal, K. Hoyt, *Otolaryngol. Head Neck Surg. (United States)*. **146**, 938–945 (2012).

158. E. J. Park, Y. Z. Zhang, N. Vykhodtseva, N. McDannold, *J. Control. Release*. **163**, 277–284 (2012).